

# Designing NSM FRP systems in concrete using partial safety factors

Mário Coelho<sup>a</sup>, Luís Neves<sup>b</sup>, José Sena-Cruz<sup>a,\*</sup>

<sup>a</sup>*ISISE, University of Minho, Department of Civil Engineering, Campus de Azurém, 4810-058 Guimarães, Portugal*

<sup>b</sup>*University of Nottingham, Department of Civil Engineering, Nottingham, United Kingdom*

---

## Abstract

This paper presents design procedures for fibre reinforced polymer (FRP) systems inserted in the cover of concrete elements according to the near-surface mounted (NSM) technique. Such strengthening system depends greatly on their bond strength. Two existing design formulations to estimate the bond strength of NSM FRP systems in concrete are studied. A reliability analysis is conducted with the purpose of making the design formulations consistent with the partial safety factors philosophy, including the Eurocodes. Hence, the necessary probabilistic distributions are calibrated based on a large database of bond tests. The results presented herein show that the existing guidelines can be extended and adopted under the framework of the Eurocodes. However, mainly due to their limitations in addressing individually all the possible failure modes, the variability of the probabilistic distributions found are quite high, leading to high partial coefficients of safety.

---

\*Corresponding author

*Email addresses:* mcoelho@civil.uminho.pt (Mário Coelho),  
luis.neves@nottingham.ac.uk (Luís Neves), jsena@civil.uminho.pt (José Sena-Cruz)

Thus, in the future, new and improved formulations should be developed.

*Keywords:* FRP, NSM, Bond, Partial Safety Factors, Reliability

---

## 1. Introduction

This work is developed within the framework of strengthening concrete structures with fibre reinforced polymers (FRP). One of the most effective techniques to do so consists on the insertion of FRP bars into grooves opened on the concrete cover of the element to be strengthened. Typically, these FRP bars are fixed to concrete with an epoxy adhesive. These procedures are commonly designated as near-surface mounted technique (NSM). Despite the progress that has been made in the past years, design formulations to safely apply NSM FRP systems in the strengthening of concrete structures are still incipient [1, 2].

One of the most critical aspects regarding the NSM technique is related to the bond behaviour of the composite system [3], i.e. the stresses transfer between concrete and the FRP reinforcing bar. To better understand that behaviour, extensive bond tests have been carried out worldwide. Despite the existence of a manifold of test setups, those can be grouped in two main types: (i) direct and (ii) beam pullout tests [1]. In this work only the first type of pullout test setup is addressed as explained in further sections.

Considering the bond behaviour of a direct pullout specimen (see an example in Fig. 1), five local failure modes can be identified. Two have cohesive nature and occur either within the adhesive layer binding FRP to concrete (A) or into the concrete surrounding the groove (C). Other two failure modes have adhesive nature since they occur in the existing two interfaces, namely,

23 between FRP and adhesive (F/A) or between adhesive and concrete (A/C).  
24 Finally, if none of the previous four failure modes occurred, failure will hap-  
25 pen by FRP tensile rupture (F) [1].

26 In a previous work, a database of each one of the referred two types  
27 of bond tests was gathered [1]. Based on it, two of the most important  
28 guidelines for the design of NSM FRP systems were tested. One guideline is  
29 proposed for the design and construction of externally bonded FRP systems  
30 for strengthening concrete structures by the American Concrete Institute [4]  
31 referred in the present paper as ACI. The other is the Design handbook for  
32 reinforced concrete structures retrofitted with FRP and metal plates: beams  
33 and slabs from Standards Australia [5], referred herein as SA. Especially, the  
34 formulations included in these two guidelines to estimate the bond strength  
35 were analysed and improvements were suggested [1].

36 According to the authors' best knowledge, nowadays there are no Eu-  
37 ropean guidelines for NSM FRP systems, even though the draft version of  
38 the new annex of EN 1992-1-1 (Eurocode 2: Part 1-1) [6] refers to NSM  
39 FRP systems. On the other hand, the formulations to estimate the bond  
40 strength of NSM FRP systems included in both ACI and SA guidelines are  
41 not consistent with the partial safety factors framework.

42 Hence, this work presents a modification of ACI and SA formulations to,  
43 consistently with the partial safety factors methodology, yield designs with  
44 acceptable reliability indexes.

45 The philosophy behind the partial safety factors method recognizes that  
46 not all the designers should be familiar with reliability concepts which, in  
47 any case, must be followed in order to have safe structures. In the partial

48 safety factor method, both actions and resistances are considered by their  
49 nominal values multiplied and divided, respectively, by partial safety factors.  
50 The way those partial factors are derived is responsible for introducing the  
51 reliability component into design. This means that, even without knowing,  
52 designers are indeed considering reliability in their projects. This philosophy  
53 is transversal to all EC thus, no matter what type of structure is being  
54 designed, the correspondent EC includes a set of partial factors to take into  
55 account the required reliability for all the design situations, designated as  
56 limit states, foreseen in that EC.

57 The Eurocode 0 (EC0) [7] describes in detail the background to the cali-  
58 bration of partial safety factors and the reliability analysis and targets used.  
59 Those are summarized in the next section.

## 60 **2. Partial safety factors method**

61 The objective of the partial safety factors method is to design structures  
62 resulting in a safety level, quantified by the reliability index, acceptable for  
63 society and similar for all types of structures. In the Eurocodes, for structures  
64 with a normal class of consequences, the target reliability index is defined  
65 equal to 3.8 for a fifty years reference period.

66 The reliability index is given by Eq. 1, where  $R$  is the resistance of the  
67 structure and  $E$  is the effect of actions. This probability can be computed  
68 using the first order reliability method (FORM). The reliability index is de-  
69 fined as the distance between the design point (i.e., the most likely failure  
70 point) and the origin in the normalized space, as shown in Fig. 2.

$$\beta = -\Phi^{-1}(p_f) = -\Phi^{-1}(P(R - E < 0)) \quad (1)$$

71 For a design corresponding to the lowest admissible value of the reliability  
 72 index, the design point has coordinates  $(-\alpha_R\beta; -\alpha_E\beta)$  in the normalized  
 73 space. The corresponding resistance in the original space is such that  $P(R =$   
 74  $R_d) = \Phi(-\alpha_R\beta)$ .

75 Although the values of the cosines  $\alpha$  vary from design to design, a value  
 76 of  $\alpha_R = 0.8$  usually leads to acceptable results. Consequently, the design  
 77 value of the resistance,  $R_d$ , can be computed according Eq. 2.

$$P(R = R_d) = \Phi(-\alpha_R\beta) = \Phi(-0.8 \times 3.8) \quad (2)$$

78 Once the probabilistic distribution of  $R$  is found, Eq. 2 can be used  
 79 directly to compute the design point and, afterwards, to define partial safety  
 80 factors that result in this design strength.

81 In the context of the present work, the partial safety factors method  
 82 was adopted to calibrate ACI and SA formulations for predicting NSM FRP  
 83 systems bond strength, using the database of direct pullout tests mentioned  
 84 previously. To do that, the following main tasks were conducted:

- 85 (i) classify the specimens according their observed experimental failure  
 86 mode and apply the corresponding theoretical limit state resistance  
 87 function ( $R_t$ ) to each specimen;
- (ii) for each specimen, estimate the error ( $\delta$ ) of the theoretical resistance  
 function using Eq. 3, where  $R_e$  is the experimental resistance value.

Then, adjust a probabilistic distribution to the theoretical resistance function errors obtained for all specimens;

$$\delta = R_e/R_t \quad (3)$$

- (iii) compute the distribution of the probabilistic resistance function ( $R$ ) defined in Eq. 4. If the only random variable in that function is the theoretical resistance function error, its probabilistic distribution can be estimated analytically. Otherwise, Monte Carlo simulation can be used to estimate the joint probabilistic distribution of all the random variables present in the probabilistic resistance function;

$$R = R_t\delta \quad (4)$$

- (iv) compute the design value of the limit state resistance function ( $R_d$ ). This should be obtained in order to have a probability of failure as defined in Eq. 5. In Eq. 5,  $\alpha_R$  is the first order reliability method sensitivity factor for resistance and  $\beta$  is the reliability index. In this work those parameters were taken as 0.8 and 3.8, respectively, according to EC0 [7] suggestion;

$$P(R = R_t\delta \leq R_d) = \Phi(-\alpha_R\beta) \quad (5)$$

- 88 (v) rewrite the resistance function in its design form and define the safety  
 89 factors to be included. This should be done taking into account that  
 90 some variables are common to other applications foreseen in the EC and  
 91 are expected to maintain the same partial safety factors throughout the  
 92 EC;

93 (vi) replace (iv) in (v) and calibrate the values of the safety factors defined  
94 in the previous step.

95 The method explained above is similar to the generic approach of the  
96 design assisted by testing method, defined in the EC0 [7]. The main difference  
97 between them is that the method presented herein uses the probabilistic  
98 models of all the random variables, which can be of any type, and Monte  
99 Carlo simulations [8] to achieve the joint probabilistic distribution of the  
100 limit state resistance function in analysis. Contrarily, the design assisted by  
101 testing method defined in the EC0 is designed for resistance functions with  
102 normal and lognormal random variables which can be handled analytically.

103 The design assisted by testing method has already been successfully used  
104 in the context of RC members with FRP internal shear reinforcement [9] or  
105 with FRP applied by the externally bonded strengthening technique either  
106 to concrete [10–13] or to masonry [14]. However, according to authors' best  
107 knowledge, this paper presents the first attempt of applying it to calibrate the  
108 reliability parameters of the bond strength resistance functions suggested by  
109 ACI and SA, including the resistance models errors. In the following sections,  
110 the major details of the application and the obtained reliability parameters  
111 are presented.

### 112 3. Data and models

113 As previously referred, a database of direct and beam pullout tests was  
114 gathered in order to assess the accuracy of ACI and SA formulations to esti-  
115 mate the bond strength of NSM FRP systems in concrete [1]. Even though  
116 not always clear, the authors of the direct pullout tests presented a single

117 critical experimental failure mode. Contrarily, in beam pullout tests, the au-  
118 thors normally provided several failure modes based on the final appearance  
119 of the tested specimen.

120 Since the failure mode needs to be clearly identified in the analyses carried  
121 herein, only direct pullout tests were selected for this study. Moreover, since  
122 the amount of tests using carbon FRP (CFRP) with rectangular cross-section  
123 is larger than the other types of FRP fibres/cross-sections, it was decided to  
124 conduct this work considering rectangular CFRP bars only.

125 Hence, [Appendix A](#) summarizes the main parameters of the 128 direct  
126 pullout tests that were used in the analyses presented in this work. They  
127 were grouped according to the failure mode obtained in the experimental  
128 tests. As it can be seen, all the possible five local failure modes (A, C, A/C,  
129 F/A and F) were found [1].

130 While in the analysis of ACI formulation all the 128 tests were used,  
131 with SA formulation some could not be used due to the lack of required  
132 information. Those specimens are identified in the notes of [Appendix A](#).

### 133 *3.1. Mechanical bond strength models*

134 Table 1 summarizes the formulations to estimate NSM FRP systems bond  
135 strength suggested by ACI and SA guidelines (see notation section for details  
136 regarding the parameters included in this table). Both formulations are based  
137 on the assumption that a minimum development length ( $L_d$ ) exists. If the  
138 existing bonded length ( $L_b$ ) is equal or larger than  $L_d$ , the maximum pullout  
139 force ( $F_{fmax}$ ) can be achieved. Otherwise, it should be reduced according to  
140 the actual bonded length.

141 ACI formulation estimates ( $F_{fmax}$ ) considering two potential failure modes.



142 The first is associated with FRP rupture. The second failure mode is related  
143 with any debonding failure of the strengthening system, thus accounting for  
144 the failure modes A, C, F/A and A/C (see Fig. 1).

145 In turn, SA formulation considers three failure modes: (i) concrete co-  
146 hesive failure; (ii) debonding failure of the strengthening system; (iii) FRP  
147 failure. Similarly to ACI formulation, the debonding failure includes failure  
148 within the adhesive or at one of the two interfaces.

149 In a previous work [1], both ACI and SA formulations were calibrated  
150 using a database of pullout tests more extensive than that used at the time  
151 both formulations were developed. Based on this, some modifications were  
152 suggested for both ACI and SA formulations in order to improve their pre-  
153 diction accuracy. Since it was proved that the pullout force depends on the  
154 FRP bar cross-section, the calibrations conducted in that work [1] considered  
155 the pullout tests separated according to the existing FRP bar cross-section.  
156 That database included pullout tests with rectangular, square and round  
157 FRP bars [1].

158 In this work, the modified ACI and SA formulations for pullout tests with  
159 FRP rectangular bars suggested in [1] were also analysed. The main purpose  
160 of this was to checking the effect of adopting more accurate formulations on  
161 the reliability analysis and partial safety factors discussed herein.

162 Regarding ACI, Coelho et al. [1] suggests that the value of the average  
163 bond strength ( $\tau_{avg}$ ) should be 9.25 MPa rather than 6.9 MPa, as recom-  
164 mended by ACI. Moreover, Coelho et al. [1] also proposed that  $\tau_{avg}$  should  
165 not be constant but, alternatively, given by the ratio between FRP cross-  
166 section area ( $A_f$ ) and the FRP/adhesive contact area, as shown in Eq. 6.

167 The latter area is defined by the product of the FRP perimeter ( $p_f$ ) and the  
168 bonded length ( $L_b$ ).

$$\tau_{avg} = 162 \left( \frac{A_f}{p_f L_b} \right)^{0.55} \quad (6)$$

169 Apart from these two differences in the assessment of  $\tau_{avg}$ , no other  
170 changes were proposed to ACI formulation. This latter formulation, using  
171 Eq. 6, will be designated as “ACI modified” herein.

172 For the case of SA, the only improvement suggested in [1] resulted from  
173 recalibrating the expressions of its original formulation. The obtained expres-  
174 sions are not reproduced herein since, as will be further explained, the results  
175 obtained in the reliability analysis with those expressions are similar to the  
176 results obtained with the original expressions suggested in SA guideline and  
177 reproduced in Table 1.

### 178 3.2. Material probabilistic models

179 In order to conduct a reliability analysis it is necessary to define the  
180 probability distribution of all random variables. Three different probability  
181 distributions are considered in this paper, namely, normal ( $N$ ), lognormal  
182 ( $LN$ ) and Weibull ( $W$ ); in what follows of this work they are presented as  
183  $N, LN$ (mean; standard deviation) and  $W(\alpha; \beta)$ , respectively. In the Weibull  
184 distribution  $\alpha$  is the scale parameter and  $\beta$  is the shape parameter.

185 It was considered that all the geometric parameters were deterministic,  
186 following the EC practice, while all mechanical parameters were considered  
187 as random variables. As shown in the previous section, ACI and SA for-  
188 mulations together require only three mechanical parameters, namely, FRP

189 modulus of elasticity ( $E_f$ ) and tensile strength ( $f_{fu}$ ) and concrete compres-  
190 sive strength ( $f_c$ ).

191 The probabilistic models for the first two parameters were obtained from  
192 the literature [15]. For both  $E_f$  and  $f_{fu}$  they consist of Weibull distributions  
193 as:

$$E_f \sim W(26.2; 180.9) \text{ GPa} \quad (7)$$

$$f_{fu} \sim W(15.9; 2777) \text{ MPa} \quad (8)$$

194 Regarding  $f_c$ , the adopted probabilistic model consisted on a lognormal  
195 distribution with 6% coefficient of variation, adapted from [16], as shown in  
196 Eq. 9. This distribution depends on the concrete class, thus the analyses  
197 were conducted taking into account the concrete mean compressive strength  
198 of each specimen according to the concrete classes defined in EC2 ( $f_{cm,EC2}$ )  
199 [6].

$$f_c \sim LN(f_{cm,EC2}; 0.06f_{cm,EC2}) \text{ MPa} \quad (9)$$

### 200 3.3. Probabilistic uncertainty for mechanical bond strength models

201 The uncertainty associated with the mechanical bond strength models,  
202 considered as a random variable, was defined by comparing the experimental  
203 maximum pullout force and the corresponding prediction according ACI and  
204 SA formulations.

205 Considering the mechanical bond models defined in section 3.1, it can  
206 be seen that, for both ACI and SA formulations, the theoretical limit state  
207 function associated with the FRP rupture (F) is defined by Eq. 10. This

208 function was applied to the 32 specimens available in the database which  
 209 presented FRP rupture failure mode.

$$R_{F(ACI/SA)} = A_f f_{fu} \quad (10)$$

210 Regarding ACI formulation, the remaining failure modes are all grouped  
 211 in the debonding limit state (B). To obtain its theoretical function, the second  
 212 branch of ACI formulation was firstly re-written by replacing  $L_d$  and  $\tau_{avg}$  in  
 213  $F_{fmax}$  expression (see Table 1), as presented in Eq. 11. This expression was  
 214 applied to the remaining 96 specimens.

$$R_{B(ACI)} = 6.9 L_b p_f \quad (11)$$

215 Regarding SA formulation, the theoretical limit state functions associated  
 216 with concrete cohesive failure (C) and debonding failures (B) were also ob-  
 217 tained by re-writing the expressions presented in Table 1 yielding to Eqs. 12  
 218 and 13, respectively. According to the failure modes reported in the database  
 219 used, these functions were applied to 35 and 39 specimens, respectively.

$$R_{C(SA)} = \sqrt{0.73 \varphi_{per}^{0.5} f_c^{0.67} L_{per} E_f A_f} \quad (12)$$

$$R_{B(SA)} = \frac{2L_b}{\pi} (0.8 + 0.078 \varphi_{per}) L_{per} f_c^{0.6} \quad (13)$$

220 In addition to ACI and SA formulations, Eq. 14, corresponding to the  
 221 ACI modified formulation referred in Eq. 6, was also used. It was applied to  
 222 the same 96 specimens as Eq. 11.

$$R_{B(ACI\ modified)} = 162 \left( \frac{A_f}{p_f L_b} \right)^{0.55} L_b p_f \quad (14)$$

223 The expressions presented above, were applied to the corresponding spec-  
224 imens and the prediction errors were estimated as the ratio between experi-  
225 mental ( $F_{fmax,Exp}$ ) and numerical ( $F_{fmax,Num}$ ) pullout forces. Then, a prob-  
226 ability distribution was fitted to the errors associated with each limit state.

227 Fig. 3 presents the probability distributions obtained for all limit state  
228 functions errors. The caption of each distribution includes also the corre-  
229 sponding probability parameters. It can be seen that, except for FRP rup-  
230 ture limit state, all other limit state errors were better fitted by lognormal  
231 distributions. This is mainly due to the asymmetry that those limit state  
232 functions present, and the need to guarantee a null probability of negative  
233 values for large coefficients of variation.

234 The coefficients of variation associated with the errors probability distri-  
235 butions were 8%, 53%, 18%, 61% and 30% for the limit states defined in Eqs.  
236 10 to 14, respectively. Those are considerably high when compared with the  
237 coefficients of variation for the materials models which were 5%, 8% and 6%,  
238 for FRP modulus of elasticity and tensile strength and concrete compressive  
239 strength, respectively.

240 The results also show that ACI modified (Eq. 14) results in a significantly  
241 lower uncertainty than the original expression proposed by ACI (Eq. 11).

#### 242 4. Safety factors calibration

243 Following the characterization of all random variables influencing the  
244 NSM FRP bond resistance, the partial safety factors were computed as de-  
245 scribed in section 2.

246 Table 2 summarizes the results obtained after applying the partial safety

247 factors method to each limit state function. In the following paragraphs some  
248 specific aspects of each limit state analysis are highlighted, while in section  
249 [5](#) a critical analysis of the obtained results is presented.

250 Regarding the FRP rupture limit state, the expression to be used in  
251 design ( $R_d$ ) is obtained from Eq. [10](#) by replacing CFRP tensile strength by  
252 its characteristic value ( $f_{fk}$ ) divided by the partial safety factor of CFRP  
253 tensile stress ( $\gamma_f$ ). This characteristic value was obtained by computing the  
254 5% quantile of Eq. [8](#).

255 Regarding both ACI and modified ACI debonding limit states (which  
256 correspond to the same physical phenomenon), since only the average bond  
257 strength is not deterministic, in the sense that it is an assumed value, the  
258 reliability of the resistance function was applied to it.

259 Both concrete cohesive failure (C) and debonding (B) limit states of SA  
260 formulation depend on the concrete class. Hence, the results of these limit  
261 states were compiled in Table [3](#) per concrete class, considering all concrete  
262 classes available in the database used. Those concrete classes were estimated  
263 on the basis that the characteristic concrete strength could be obtained by  
264 subtracting 8 MPa to its mean value (provided by the authors of the exper-  
265 imental studies and shown in the [Appendix A](#) for each specimen) [[6](#)].

266 In both C and B limit states of SA formulation, the expression to be used  
267 in design is similar to their corresponding theoretical limit state functions.  
268 The only two differences are that concrete mean strength was replaced by its  
269 characteristic value ( $f_{ck}$ ) divided by concrete's partial safety factor ( $\gamma_c = 1.5$ )  
270 [[6](#)] and that a new safety factor was added in each expression. This parameter  
271 behaves as a global safety factor and was computed per concrete class. The

272 obtained values were also shown in Table 3.

#### 273 4.1. Proposed design formulations

274 With the reliability parameters calibrated in the previous section, the  
 275 expressions of ACI formulation presented in Table 1 should be replaced by  
 276 Eqs. 15 and 16, in which  $\gamma_f = 1.4$  and  $\tau_d = 1.77$  MPa. Regarding the  
 277 ACI modified formulation the only difference is that  $\tau_d$  should be defined  
 278 according to Eq. 17.

$$L_d = \frac{A_f \frac{f_{fk}}{\gamma_f}}{p_f \tau_d} \quad (15)$$

$$F_{fmax,d} = \begin{cases} A_f \frac{f_{fk}}{\gamma_f} & \text{if } L_b \geq L_d \\ A_f \frac{f_{fk}}{\gamma_f} \frac{L_b}{L_d} & \text{if } L_b < L_d \end{cases} \quad (16)$$

$$\tau_d = 61.6 \left( \frac{A_f}{p_f L_b} \right)^{0.55} \quad (17)$$

279 Similarly, SA formulation should be applied using Eqs. 18 to 20 to replace  
 280 the corresponding ones in Table 1. In these equations  $\gamma_f = 1.4$  and the  
 281 parameters  $\eta_c$  and  $\eta_b$  should be taken from Table 3.

$$\tau_d = (0.8 + 0.078 \varphi_{per}) \left( \frac{f_{ck}}{\gamma_c} \right)^{0.6} \quad (18)$$

$$\delta_d = \left[ 0.73 \varphi_{per}^{0.5} \left( \frac{f_{ck}}{\gamma_c} \right)^{0.67} \right] / \tau_d \quad (19)$$

$$F_{fmax,d} = \begin{cases} \eta_c \sqrt{\tau_d \delta_d L_{per} E_f A_f} \leq A_f \frac{f_{fk}}{\gamma_f} & \text{if } L_b \geq L_d \\ \eta_b \sqrt{\tau_d \delta_d L_{per} E_f A_f} \frac{L_b}{L_d} \leq A_f \frac{f_{fk}}{\gamma_f} & \text{if } L_b < L_d \end{cases} \quad (20)$$

## 282 5. Results analysis

283 The results obtained in the reliability analysis presented in the previous  
284 sections are discussed in the following. The discussion begins by presenting in  
285 Section 5.1 the performance of the guidelines' original formulations in terms  
286 of failure mode prediction. Then, the remaining sections detail the major  
287 aspects related with the reliability analysis.

### 288 5.1. Specimens separated by guidelines' failure mode

289 According to EC philosophy, a theoretical resistance function should be  
290 developed based on the physics of the phenomenon in analysis. This means  
291 that the developed theoretical resistance function should be capable of pre-  
292 dicting the real failure mode, even if the predicted strength results inaccurate.

293 To verify that aspect, both ACI and SA formulations as defined in the  
294 corresponding guidelines were applied to the database. Fig. 4 presents a  
295 comparison between the failure modes obtained in the experimental pullout  
296 tests (horizontal axis) and those predicted by ACI and SA guidelines (vertical  
297 axis). As can be seen, while in the experimental tests all the possible five  
298 failure modes occurred, in the guidelines' predictions only two failure modes  
299 were observed (F or B in ACI and C or B in SA). Remind that whilst this  
300 corresponds to all the failure modes that ACI considers, in the case of SA,  
301 the failure by FRP rupture was not predicted in any test.

302 Regarding ACI, it can be seen that its predictions fail more frequently  
303 when the real failure occurs by FRP rupture than when it occurs by one of the  
304 other four failure modes (all grouped in the debonding failure mode of ACI).  
305 Taking into account that the failure by FRP rupture is expected to occur for



306 the highest pullout force that a specimen can sustain [1], when ACI predicts  
307 debonding and the real failure mode was FRP rupture, the prediction can  
308 be considered safe. Contrarily, when ACI predicts FRP rupture and the  
309 real failure occurred by any debonding mechanism, the prediction is unsafe.  
310 Hence, even though ACI fails more frequently when the real failure mode  
311 is FRP failure, the major problem is related with those specimens in which  
312 ACI predicted debonding failure and it actually occurred by FRP rupture.

313 Regarding SA, the first aspect to be mentioned is that, even though there  
314 are 32 specimens failing by FRP rupture in the database used, SA formula-  
315 tion did not predict any FRP rupture. Considering that the concrete failure  
316 is expected to occur for pullout forces larger than those occurring for any  
317 debonding failure (in SA this includes A, F/A and A/C) [1], the main prob-  
318 lem regarding this formulation is also related with the prediction of debonding  
319 failure mode. In fact, there are several specimens in which the failure oc-  
320 curred by one of the three debonding mechanisms and SA predicted a failure  
321 within concrete.

## 322 *5.2. Specimens separated by experimental failure mode*

323 As already mentioned, a reliability analysis must be conducted taking  
324 into account the real failure mode occurred in each specimen. Hence, the  
325 specimens presented in [Appendix A](#) were separated by experimental failure  
326 mode regardless to the fact that, as referred in the previous section, the  
327 guidelines predict different failure modes in many cases.

328 Fig. 5 presents the relationship between experimental pullout force and  
329 that foreseen by each guideline for each specimen. Note that the later was  
330 obtained by applying directly the limit state function corresponding to the

331 experimental failure mode and not the formulation as described in each guide-  
332 line.

333 For both guidelines it can be seen that the limit state function related  
334 with FRP rupture (F) is the one presenting the lowest dispersion in the  
335 predictions. In the case of SA formulation, this dispersion was followed by the  
336 limit state functions for concrete cohesive failure (C) and, finally, debonding  
337 failure (B).

338 The limit state function associated with FRP rupture in NSM FRP sys-  
339 tems coincides with the limit state function for the FRP rupture in tensile  
340 tests of FRP bars alone. The latter can be estimated using a classical and  
341 well established mechanical model (the product of the bar cross-section area  
342 by its normal strength). Hence, in this case, the dispersion of results should  
343 be mainly related with the different support conditions that exist in NSM  
344 FRP pullout tests when compared with those of a tension FRP bar test  
345 (together with the uncertainty in FRP mechanical properties).

346 The debonding limit state function addresses several failures using a single  
347 expression. Since the debonding mechanisms associated with each of these  
348 debonding failure modes are different, it is expectable that the same function  
349 predicts more accurately one of them and less accurately the remaining ones.  
350 This conclusion can be shown with the results in Fig. 5b. Since SA has  
351 an individual limit state function for concrete failure, its dispersion is lower  
352 than that found for debonding failures. Moreover, since ACI debonding limit  
353 state function addresses four failure modes while in SA it addresses three, the  
354 dispersion of predictions is larger in the former (Fig. 5a) than in the latter  
355 (Fig. 5b). This, naturally, has implications on the partial safety factors that

356 were determined.

### 357 5.3. Bond strength according to the theoretical resistance models

358 Again according to the principals defined in EC0 [7], a theoretical resis-  
359 tance function should be capable of predicting the phenomenon it is repre-  
360 senting on average. This means that, the value of the theoretical resistance  
361 function error ( $\delta$ ), expressed as the ratio between experimental ( $F_{fmax,Exp}$ )  
362 and numerical ( $F_{fmax,Num}$ ) pullout forces, should have an average equal to  
363 one, being its distribution approximately symmetric. Fig. 6 presents the  
364 referred error obtained after applying both guideline's formulations to the  
365 database in Appendix A (red bars in each figure).

366 In both ACI (Fig. 6a) and SA (Fig. 6b) guidelines, about  $\frac{1}{3}$  of predictions  
367 have a ratio inferior to one while the remaining  $\frac{2}{3}$  stand above one. This  
368 means that both formulations are conservative, eventually already including  
369 some type of safety factors while those should be obtained *a posteriori*.

370 Contrarily, the modification proposed by the authors for ACI formulation  
371 (Fig. 6c) presents 45% and 55% of the predictions equal or below and above  
372 the unit, respectively, resulting in a centred prediction.

### 373 5.4. Partial safety factor for CFRP ( $\gamma_f$ )

374 From the available data the 32 specimens that failed by FRP rupture were  
375 used in the calibration of  $\gamma_f$ . Since both ACI and SA formulations present  
376 the same function for this limit state, a single value of  $\gamma_f = 1.4$  was obtained  
377 for both guidelines.

378 According to EC philosophy, each material should have a single partial  
379 safety factor to be used in all the situations where that material can be

380 applied and regardless to the resistance model being used. The obtained  $\gamma_f$   
381 matches that requirement.

382 The value of  $\gamma_f$  found herein corresponds to an upper bound of those  
383 suggested in the literature. According to the authors' best knowledge, there  
384 are only two guidelines for the strengthening of concrete structures with FRP  
385 systems in which values of  $\gamma_f$  are explicitly provided.

386 The first one, referred herein as Italian guideline [17], addresses the  
387 strengthening using the externally bonded technique. It presents values of  
388  $\gamma_f$  depending on the type of failure mode that can be influenced by the FRP  
389 properties. Hence, if the relevant failure mode is by FRP rupture (which is  
390 influenced by FRP properties) then its  $\gamma_f$  can be 1.1 or 1.25, depending on  
391 the type of certification of the strengthening system. If the critical failure  
392 mode is by debonding,  $\gamma_f$  can be 1.2 or 1.5, again depending on the certifi-  
393 cation type. Even though a single value should exist for  $\gamma_f$ , the authors of  
394 the Italian guideline decided for the use of different values for different limit  
395 states. Nevertheless, the important aspect is that the value suggested herein  
396 is in the range of those suggested by the Italian guideline thus harmonization  
397 of  $\gamma_f$  value could be easily achieved in the future.

398 The second guideline, is the Canadian Highway Bridge Design Code [18].  
399 This guideline presents the values for  $\gamma_f$  in the form of a global factor to be  
400 applied to FRP tensile strength. It suggests the use of 0.85 for Aramid and  
401 Carbon FRP and 0.75 for glass FRP, corresponding to  $\gamma_f$  of 1.18 and 1.33,  
402 respectively, which are also similar to the value of 1.4 suggested herein.

403 *5.5. ACI debonding safety factor ( $\tau_d$ )*

404     Regarding the debonding limit state defined by ACI guideline it was de-  
405 cided to guarantee the required safety margin by reducing the bond strength.  
406 This resulted in replacing the value of the average bond strength proposed  
407 in ACI,  $\tau_{avg} = 6.9$  MPa, by its design value  $\tau_d = 1.77$  MPa, calibrated in sec-  
408 tion 4. As referred before, this very large decrease (about 70%) in the bond  
409 strength results from the large uncertainty in the prediction models, a con-  
410 sequence of having a single expression addressing four different phenomena.  
411 Besides, as discussed in [1], the use of a single bond strength value, regardless  
412 of the FRP cross-section type, introduces a higher level of uncertainty than  
413 when the bond strength is estimated as a function of the FRP cross-section.

414     To verify that, the alternative designated ACI modified was also tested  
415 in this work (see section 4). The design bond strength obtained with that  
416 different and more accurate model was about 60% lower than the original  
417 value. This smaller reduction proves that, even if a single limit state function  
418 is used to address all four failure modes, a more accurate prediction model  
419 can result in a significant increase in design strength.

420 *5.6. SA global safety factors ( $\eta_c$  and  $\eta_b$ )*

421     Regarding SA limit states related with concrete and debonding failure  
422 modes, it was decided to provide them with reliability features by applying  
423 global safety factors. The reason for this decision is related with the type  
424 of variables their resistance functions include. Besides geometry variables,  
425 which are treated as deterministic, both resistance functions contain two  
426 mechanical variables only. Namely, the compressive strength of concrete and  
427 the FRP modulus of elasticity (just in concrete limit state).

428        Regarding concrete compressive strength, it already has a well-established  
429 partial safety factor of 1.5 which, according to EC philosophy, should be  
430 maintained in all the applications of concrete material. Regarding the FRP  
431 modulus of elasticity, it is not usual to affect the elasticity modulus of a ma-  
432 terial with partial factors. Instead, the usual procedure consists on applying  
433 such factors to material's stresses and strains thus, by Hooke's law, the elas-  
434 ticity modulus remains unaffected by safety factors. In order to maintain this  
435 approach, thus addressing the compatibility between codes recommended by  
436 EC, it was also decided to do not apply partial safety factor to the FRP  
437 modulus of elasticity.

438        Hence, the solution adopted was the use of global safety factors as defined  
439 in section 4 for concrete and debonding limit states. As expected, comparing  
440 the magnitude of values obtained, it can be seen that the safety factors are  
441 lower for debonding than for concrete limit state. This is mainly related with  
442 the former addressing several failure modes, as mentioned before.

443        For design purposes it would be better to have a single global safety  
444 factor for each limit state, regardless to the concrete class. In fact, EC also  
445 presents a single partial safety factor for concrete regardless to its class. On  
446 the other hand, the global safety factors obtained herein (see Table 3) are  
447 quite similar, thus the lowest value of each safety factor can be used for each  
448 limit state and for all concrete classes. The impact of this option would be  
449 a more conservative design for those specimens using concrete classes bellow  
450 C55/67, which is the class presenting the lowest global safety factors.

451 *5.7. Bond strength in the theoretical resistance models with reliability param-*  
452 *eters*

453 Contrarily to what was referred before for the theoretical models, the  
454 models with reliability parameters are not expected to necessarily predict  
455 the real failure mode. In fact, these models will produce prediction values  
456 lower than the real ones, thus safer.

457 Fig. 6 presents, as blue bars, the ratio between the experimental maxi-  
458 mum pullout force and that estimated using the proposed design formulations  
459 (including the corresponding safety factors). The obtained results show, as  
460 expected, that all these ratios are larger than one. The only exception occurs  
461 for SA guideline (see Fig. 6b) where only one specimen attained a ratio of  
462 0.94 mainly due to decimals rounding.

463 Comparing the magnitude of the ratios obtained, those are in agreement  
464 with the reliability parameters estimated for each formulation. The higher  
465 the reductions applied to each limit state function, the larger the ratios are. It  
466 should be mentioned that, from a design viewpoint, larger ratios correspond  
467 to less economical designs, thus it would be better if the ratios were as small  
468 as possible, yet larger than one.

469 Concerning ACI formulation as defined in the guideline (Fig. 6a) or its  
470 modified version (Fig. 6c), it can be confirmed that the lower reduction on  
471 the design bond strength associated with the better accuracy of the latter,  
472 resulted in less conservative predictions. In other words, the blue bars in Fig.  
473 6a present a larger dispersion and are available in larger numbers in the right  
474 side of the figure than the ones shown in Fig. 6c.

475 Regarding SA guideline (Fig. 6b), the ratios are lower than 2.5 for about

476 40% of the specimens while for the remaining specimens the ratios increase  
477 up to 16.5. This should be related with the global reliability parameters  
478 applied for concrete and debonding failure limit states in SA formulation.  
479 In fact, the reductions applied to these limit states were as high as 35%  
480 and 77% of their theoretical prediction, respectively. This emphasizes the  
481 fact that safety factors should be applied to individual material properties,  
482 rather than to the entire resistance function.

### 483 5.8. Probability models adopted for CFRP parameters

484 Despite the considerable range of the two CFRP properties required  
485 in the resistance models analysed in this work ( $E_f = [123 - 182]$  GPa,  
486  $f_{fu} = [1850 - 3100]$  MPa), the same model was used for each parameter  
487 and for all specimens. Even though this could seem to be a limitation of  
488 the present study, the range of values referred above are within the range of  
489 values used in the development of the probabilistic models for CFRP prop-  
490 erties used herein. Eqs. 7 and 8 were defined by using CFRP bars with  $E_f$   
491 ranging between 118 to 218 GPa and  $f_{fu}$  ranging between 1780 to 3310 MPa  
492 [15]. Note that these CFRP bars correspond to a single brand from a single  
493 manufacturer. However, assuming that the production processes adopted by  
494 different manufacturers would be similar, the coefficients of variation regard-  
495 ing  $E_f$  and  $f_{fu}$  for other CFRP bars' brands, should be also similar, differing  
496 mainly in the average values.

497 It has been proved that CFRP tensile properties ( $E_f$  and  $f_{fu}$ ) are well  
498 described by Weibull probability distributions [15, 19–21], which have a co-  
499 efficient of variation,  $c_v$ , estimated according Eq. 21, where  $\Gamma$  is the Gamma  
500 function and  $\alpha$  is the Weibull distribution scale parameter. In the Weibull



501 distributions presented in Eqs. 7 and 8 it can be seen that the shape param-  
502 eter  $\beta$  (which does not appear in the expression of  $c_v$ ) roughly coincides with  
503 the average value of each property.

$$c_v = \frac{\sqrt{\Gamma\left(1 + \frac{2}{\alpha}\right) - \Gamma^2\left(1 + \frac{1}{\alpha}\right)}}{\Gamma\left(1 + \frac{1}{\alpha}\right)} \quad (21)$$

504 Taking all of these into account, it can be assumed that since differ-  
505 ent CFRP brands would have different mechanical properties average values  
506 (related with the material composition) but similar coefficients of variation  
507 (related with the fabrication process), and that the average value has no  
508 influence on the coefficient of variation, the same model can be used for  
509 different CFRP brands, which validates the analyses presented in this work.

510 In any case, the results obtained in this work were found satisfactory. In  
511 the future, as new probabilistic models for these CFRP parameters become  
512 available, the analyses presented herein can be easily updated and these  
513 assumptions validated.

#### 514 *5.9. Influence of the mechanical model*

515 As referred in section 3.1, in a previous work both ACI and SA were  
516 recalibrated [1]. Namely, in the case of ACI formulation its average bond  
517 strength value was recalibrated. In the case of SA formulation the expressions  
518 that were developed by SA authors based on experimental data were also  
519 recalibrated. This includes the expressions for  $\tau_{max}$  and  $\delta_{max}$  (see Table 1).

520 These recalibrated formulations were also object of a reliability analysis  
521 using the methodology described in this work.

522 Regarding ACI, the recalibrated average bond strength value was equal

523 to 9.25 MPa. As expected, it was found that the use of this value in the  
524 theoretical resistance function lead to the same value of  $\tau_d = 1.77$  MPa in  
525 the design function. In fact, using 9.25, 6.9 or any other scalar as theoret-  
526 ical average bond strength, would lead to the same average bond strength  
527 design value. Using different scalars, one is just shifting the mean of the  
528 error being the coefficient of variation the same. Hence, unless the latter,  
529 which is the important statistical parameter in the reliability analyses, sig-  
530 nificantly changes, the design value would always be the same regardless to  
531 the theoretical value adopted.

532 An example of that change could be achieved by replacing the scalar av-  
533 erage bond strength by an expression. That was already verified before when  
534 the ACI modified version was presented. In the end, the resistance design  
535 values obtained for ACI formulation with any scalar (6.9, 9.25, ... MPa) was  
536 always 0.26 while it increased to 0.39 for ACI modified version.

537 Regarding SA, the recalibrated expressions lead also to similar design  
538 values. In fact, the mechanical models were the same, but with lower average  
539 prediction errors. Hence, only the original version of this formulation was  
540 referred in the previous sections.

## 541 **6. Conclusions**

542 This paper presented a reliability analysis over two of the most important  
543 guidelines for the design of concrete structures strengthened with NSM FRP  
544 systems. A formulation for calibrating the reliability parameters necessary  
545 to make the referred guidelines consistent with the partial safety factors  
546 philosophy was shown and the correspondent reliability parameters deduced.

547 From the work presented herein, the following major conclusions can be  
548 drawn:

- 549 • the absence of probabilistic models for the different types of FRP lim-  
550 ited this study to carbon FRP. A large scale analysis of the probabilis-  
551 tic models for FRP properties is paramount for defining reliable design  
552 codes;
- 553 • the amount of experimental data available is still very low. This has  
554 direct influence in the definition of the errors associated with each  
555 limit state function. For this reason, in this work only direct pull-  
556 out specimens with CFRP rectangular bars were considered. Hence, it  
557 is necessary to continue performing direct pullout tests, specially using  
558 combinations of parameters and materials that were not tested yet;
- 559 • due to the non-existence of a standard NSM FRP direct pullout test,  
560 part of the theoretical resistance models errors should be associated  
561 with the differences between tests conditions rather than with the mod-  
562 els. In fact, aspects like specimen size, setup configuration or even  
563 support conditions could influence the experimental maximum pullout  
564 force value. That will naturally also influence the magnitude of the  
565 errors associated with the perdition models. Hence, the definition of a  
566 standard NSM FRP direct pullout test is urgent;
- 567 • while in the case of ACI formulation it was possible to define reliabil-  
568 ity parameters affecting directly specific properties (either FRP tensile  
569 strength or strengthening system bond strength), in the case of SA the  
570 reliability had to be included by means of global safety factors in order

571 to maintain the partial safety factor of concrete in agreement with that  
572 already in the Eurocodes;

573 • it was confirmed that, mainly due to the difficulty of ACI and SA  
574 guidelines to predict separately all the five local failure modes existing  
575 in a NSM FRP system, more accurate resistance models should be  
576 developed for estimating the bond strength of NSM FRP systems in  
577 the future;

578 • finally, regardless to the limitations of ACI and SA guidelines, the  
579 necessary reliability parameters were estimated and can be used in  
580 order to design NSM FRP systems according to Eurocodes philosophy,  
581 thus attaining a strengthening with the reliability index recommended  
582 by Eurocodes.

### 583 **Acknowledgements**

584 This work was supported by FEDER funds through the Operational Pro-  
585 gram for Competitiveness Factors – COMPETE and National Funds through  
586 FCT (Portuguese Foundation for Science and Technology) under the project  
587 CutInDur FCOMP-01-0124-FEDER-014811 (ref. PTDC/ECM/112396/2009)  
588 and partly financed by the project POCI-01-0145-FEDER-007633. The first  
589 author wishes also to acknowledge the Grant No. SFRH/BD/87443/2012  
590 provided by FCT.

591 **Appendix A.**

592 The following table contains the data used in the analyses presented in this paper.

Paper ID	Specimen ID	$b_g$ [mm]	$d_g$ [mm]	$L_b$ [mm]	$f_{cm}$ [MPa]	$p_f$ [mm]	$A_f$ [mm <sup>2</sup> ]	$E_f$ [GPa]	$f_{fu}$ [MPa]	$F_{fmax}$ [kN]
FRP tensile rupture failure mode, F (32 specimens)										
[22]	48 MPa-200-10	3.28	12.10	200.00	48.20	22.76	12.93	161.80	2643.00	33.70
[22]	49 MPa-200-10	3.26	12.56	200.00	49.20	23.64	13.31	161.80	2643.00	33.30
[22]	49 MPa-200-20	3.28	22.43	200.00	49.20	43.42	26.15	162.30	2796.00	68.60
[22]	49 MPa-300-20	3.24	21.79	300.00	49.20	42.06	24.54	162.30	2796.00	68.10
[22]	53 MPa-200-20	3.26	22.47	200.00	52.80	43.46	25.79	162.30	2796.00	77.90
[22]	53 MPa-200-20	3.27	22.10	200.00	53.00	42.74	25.53	162.30	2796.00	72.50
[22]	53 MPa-100-10	3.26	12.37	100.00	53.00	23.26	13.07	161.80	2643.00	29.50
[22]	53 MPa-300-10	3.27	12.30	300.00	53.00	23.14	13.08	161.80	2643.00	37.90
[22]	53 MPa-300-20	3.25	22.15	300.00	53.00	42.80	25.19	162.30	2796.00	66.30
[22]	33 MPa-300-20	3.24	21.85	300.00	33.40	42.18	24.61	162.30	2796.00	67.80
[23]	C-1.4x10-S-1	5.00	15.00	300.00	18.40	22.80	14.00	177.00	2221.00	31.16
[23]	C-1.4x10-S-2	5.00	15.00	300.00	18.40	22.80	14.00	177.00	2221.00	32.93
[23]	C-1.4x10-S-3	5.00	15.00	300.00	18.40	22.80	14.00	177.00	2221.00	34.73

*Continued on next page*

*Continued from previous page*

Paper ID	Specimen ID	$b_g$ [mm]	$d_g$ [mm]	$L_b$ [mm]	$f_{cm}$ [MPa]	$p_f$ [mm]	$A_f$ [mm <sup>2</sup> ]	$E_f$ [GPa]	$f_{fu}$ [MPa]	$F_{fmax}$ [kN]
[24]	8-31[R/60/L/6.4p]	10.00	24.00	230.00	56.24	36.00	32.00	123.00	2043.00	61.60
[24]	8-31[R/60/L/6.4p]c	10.00	24.00	230.00	56.24	36.00	32.00	123.00	2043.00	62.10
[25]	Lb90X12_a	5.00	22.00	90.00	25.03	22.02	13.86	156.10	2879.00	37.32
[25]	Lb90X12_b	5.00	22.00	90.00	25.03	22.02	13.86	156.10	2879.00	34.61
[25]	Lb120X12_a	5.00	22.00	120.00	25.03	22.02	13.86	156.10	2879.00	37.95
[25]	Lb150X12_b	5.00	22.00	150.00	25.03	22.02	13.86	156.10	2879.00	38.39
[25]	Lb90X6_a	5.00	22.00	90.00	25.03	22.02	13.86	156.10	2879.00	34.38
[25]	Lb90X6_b	5.00	22.00	90.00	25.03	22.02	13.86	156.10	2879.00	33.50
[25]	Lb120X6_a	5.00	22.00	120.00	25.03	22.02	13.86	156.10	2879.00	36.15
[25]	Lb120X6_a	5.00	22.00	120.00	25.03	22.02	13.86	156.10	2879.00	34.26
[25]	Lb150X6_b	5.00	22.00	150.00	25.03	22.02	13.86	156.10	2879.00	36.47
[25]	Lb120X0_a	5.00	22.00	120.00	25.03	22.02	13.86	156.10	2879.00	33.78
[25]	Lb120X0_b	5.00	22.00	120.00	25.03	22.02	13.86	156.10	2879.00	35.39
[25]	Lb150X0_a	5.00	22.00	150.00	25.03	22.02	13.86	156.10	2879.00	37.29
[25]	Lb150X0_b	5.00	22.00	150.00	25.03	22.02	13.86	156.10	2879.00	32.05

*Continued on next page*

Continued from previous page

Paper ID	Specimen ID	$b_g$ [mm]	$d_g$ [mm]	$L_b$ [mm]	$f_{cm}$ [MPa]	$p_f$ [mm]	$A_f$ [mm <sup>2</sup> ]	$E_f$ [GPa]	$f_{fu}$ [MPa]	$F_{fmax}$ [kN]
[26]*	TS1-3.6-C20	NA	25.00	350.00	38.80	27.20	36.00	165.00	2700.00	79.60
[26]*	TS1-3.6-C20R	NA	25.00	350.00	38.80	27.20	36.00	157.00	2700.00	95.00
[26]*	TS1-3.6-C30	NA	35.00	350.00	38.80	27.20	36.00	156.00	2700.00	101.80
[26]*	TS1-3.6-C40	NA	45.00	350.00	38.80	27.20	36.00	160.00	2700.00	105.70
Cohesive failure mode at concrete, C (50 specimens)										
[22]	30 MPa-100-10b	3.20	12.00	100.00	30.00	22.40	12.00	161.80	2643.00	22.60
[22]	30 MPa-100-10	3.22	12.02	100.00	30.00	22.48	12.22	161.80	2643.00	20.40
[22]	30 MPa-150-10	3.23	12.33	150.00	30.00	23.12	12.71	161.80	2643.00	23.20
[22]	30 MPa-200-10	3.22	12.48	200.00	30.00	23.40	12.79	161.80	2643.00	27.90
[22]	30 MPa-250-10	3.22	12.29	250.00	30.00	23.02	12.55	161.80	2643.00	26.60
[22]	30 MPa-300-10	3.22	12.38	300.00	30.00	23.20	12.66	161.80	2643.00	26.00
[22]	30 MPa-350-10	3.22	12.35	350.00	30.00	23.14	12.63	161.80	2643.00	23.00
[22]	42 MPa-200-10	3.27	12.29	200.00	41.80	23.12	13.07	161.80	2643.00	30.60
[22]	30 MPa-100-20	3.20	22.00	100.00	30.00	42.40	24.00	162.30	2796.00	51.40
[22]	30 MPa-200-20	3.20	22.00	200.00	30.00	42.40	24.00	162.30	2796.00	57.80

Continued on next page

*Continued from previous page*

Paper ID	Specimen ID	$b_g$ [mm]	$d_g$ [mm]	$L_b$ [mm]	$f_{cm}$ [MPa]	$p_f$ [mm]	$A_f$ [mm <sup>2</sup> ]	$E_f$ [GPa]	$f_{fu}$ [MPa]	$F_{fmax}$ [kN]
[22]	30 MPa-300-20	3.20	22.00	300.00	30.00	42.40	24.00	162.30	2796.00	66.70
[22]	65 MPa-200-10	4.88	12.08	200.00	64.80	25.92	29.03	144.60	2634.00	45.00
[22]	65 MPa-200-20	4.97	21.77	200.00	64.80	45.48	58.72	162.30	2796.00	108.80
[22]	53 MPa-200-10	3.24	12.23	200.00	52.80	22.94	12.69	161.80	2643.00	31.90
[22]	53 MPa-200-10	3.30	12.43	200.00	53.00	23.46	13.56	161.80	2643.00	34.00
[22]	53 MPa-100-20	3.25	22.23	100.00	53.00	42.96	25.29	162.30	2796.00	63.80
[22]	33 MPa-200-15	3.26	17.65	200.00	33.40	33.82	19.72	162.05	2643.00	47.10
[22]	33 MPa-300-15	3.26	17.31	300.00	33.40	33.14	19.29	162.05	2643.00	51.60
[22]	65 MPa-200-10	4.90	11.95	200.00	64.80	25.70	28.86	144.60	2634.00	45.10
[22]	33 MPa-200-20	3.20	22.00	200.00	33.40	42.40	24.00	162.30	2796.00	52.40
[27]	P2	5.00	20.00	300.00	50.00	36.00	45.00	157.00	2580.00	57.30
[27]	P4	5.00	20.00	300.00	50.00	36.00	45.00	157.00	2580.00	56.74
[27]	P6	5.00	25.00	300.00	50.00	45.00	50.00	153.00	2500.00	62.40
[28]	E-RT-1	6.40	21.00	152.00	40.70	36.00	32.00	141.50	2775.50	50.60
[28]	E-RT-2	6.40	21.00	152.00	40.70	36.00	32.00	141.50	2775.50	52.20

*Continued on next page*



*Continued from previous page*

Paper ID	Specimen ID	$b_g$ [mm]	$d_g$ [mm]	$L_b$ [mm]	$f_{cm}$ [MPa]	$p_f$ [mm]	$A_f$ [mm <sup>2</sup> ]	$E_f$ [GPa]	$f_{fu}$ [MPa]	$F_{fmax}$ [kN]
[28]	E-RT-3	6.40	21.00	152.00	40.70	36.00	32.00	141.50	2775.50	55.40
[28]	E-RT-4	6.40	21.00	152.00	40.70	36.00	32.00	141.50	2775.50	55.70
[29]	G0NSM1	3.00	21.00	350.00	35.50	42.40	24.00	161.00	2720.00	61.20
[29]	G0NSM2	3.00	21.00	350.00	35.50	42.40	24.00	161.00	2720.00	64.80
[30]	N150-1	7.10	20.00	150.00	24.00	39.20	57.60	160.00	2800.00	88.26
[30]	N200-1	7.10	20.00	200.00	24.00	39.20	57.60	160.00	2800.00	90.21
[25]	Lb70X0_a	5.00	22.00	70.00	25.03	42.80	28.00	165.00	1850.00	36.53
[25]	Lb70X0_b	5.00	22.00	70.00	25.03	42.80	28.00	165.00	1850.00	34.58
[25]	Lb90X0_a	5.00	22.00	90.00	25.03	42.80	28.00	165.00	1850.00	42.00
[25]	Lb90X0_b	5.00	22.00	90.00	25.03	42.80	28.00	165.00	1850.00	41.70
[29]**	C150NSMb	NA	NA	350.00	35.50	84.80	96.00	173.00	2720.00	205.10
[26]**	TS1-3.6-C0	NA	5.00	350.00	38.80	27.20	36.00	150.00	2700.00	40.00
[26]**	TS1-3.6-C0R	NA	5.00	350.00	38.80	27.20	36.00	160.00	2700.00	39.20
[26]**	TS1-3.6-C10	NA	15.00	350.00	38.80	27.20	36.00	165.00	2700.00	61.80
[26]**	TS2-6.0-C0	NA	5.00	350.00	38.80	32.00	60.00	166.00	2700.00	54.80

*Continued on next page*

*Continued from previous page*

Paper ID	Specimen ID	$b_g$ [mm]	$d_g$ [mm]	$L_b$ [mm]	$f_{cm}$ [MPa]	$p_f$ [mm]	$A_f$ [mm <sup>2</sup> ]	$E_f$ [GPa]	$f_{fu}$ [MPa]	$F_{fmax}$ [kN]
[26]**	TS2-6.0-C10	NA	15.00	350.00	38.80	32.00	60.00	165.00	2700.00	86.10
[26]**	TS2-6.0-C20	NA	25.00	350.00	38.80	32.00	60.00	169.00	2700.00	136.00
[26]**	TS2-6.0-C30B	NA	35.00	350.00	38.80	32.00	60.00	159.00	2700.00	108.80
[26]**	TS2-6.0-C50	NA	55.00	350.00	38.80	32.00	60.00	NA	2700.00	81.80
[26]**	TS2-6.0-C55	NA	60.00	350.00	38.80	32.00	60.00	160.00	2700.00	138.20
[26]**	TS3-6.0-C15	NA	20.00	350.00	38.80	32.00	60.00	160.00	2700.00	89.80
[26]**	TS3-6.0-C25	NA	30.00	350.00	38.80	32.00	60.00	161.00	2700.00	117.00
[26]**	TS3-6.0-C30	NA	35.00	350.00	38.80	32.00	60.00	160.00	2700.00	129.90
[26]**	TS3-6.0-C40	NA	45.00	350.00	38.80	32.00	60.00	154.00	2700.00	130.60
[26]**	TS3-6.0-C50	NA	45.00	350.00	38.80	32.00	60.00	NA	2700.00	90.00
Cohesive failure mode at adhesive, A (10 specimens)										
[22]	49 MPa-100-20	3.27	22.37	100.00	49.20	43.28	25.87	162.30	2796.00	64.10
[22]	49 MPa-200-20	3.28	22.22	200.00	49.20	43.00	25.88	162.30	2796.00	75.00
[22]	33 MPa-100-15	3.26	16.93	100.00	33.40	32.38	18.81	162.05	2643.00	31.90
[31, 32]	C_STR_2x16	8.00	25.00	300.00	35.00	36.00	32.00	124.00	2068.00	46.50

*Continued on next page*

Continued from previous page

Paper ID	Specimen ID	$b_g$ [mm]	$d_g$ [mm]	$L_b$ [mm]	$f_{cm}$ [MPa]	$p_f$ [mm]	$A_f$ [mm <sup>2</sup> ]	$E_f$ [GPa]	$f_{fu}$ [MPa]	$F_{fmax}$ [kN]
[24]	7-25[R/60/S/1.6p]	6.00	20.00	58.00	57.52	36.00	32.00	123.00	2043.00	28.10
[24]	7-26[R/60/S/3.2p]	6.00	20.00	115.00	55.68	36.00	32.00	123.00	2043.00	34.30
[24]	7-27[R/60/S/6.4p]	6.00	20.00	230.00	55.68	36.00	32.00	123.00	2043.00	50.80
[24]	7-28[R/60/S/12.7p]	6.00	20.00	460.00	49.92	36.00	32.00	123.00	2043.00	57.10
[24]	8-29[R/60/L/1.6p]	10.00	24.00	58.00	56.24	36.00	32.00	123.00	2043.00	26.20
[24]	8-30[R/60/L/3.2p]	10.00	24.00	115.00	57.52	36.00	32.00	123.00	2043.00	43.40
FRP/Adhesive interface failure mode, F/A (19 specimens)										
[33]	CS-200	9.00	22.00	200.00	23.20	40.00	64.00	151.00	2068.00	54.50
[33]	CS-250	9.00	22.00	250.00	23.20	40.00	64.00	151.00	2068.00	64.00
[31, 32]	C-2.5x15-S1	8.00	25.00	300.00	34.00	35.00	37.50	165.00	3100.00	60.60
[31, 32]	C-2.5x15-S2	8.00	25.00	300.00	34.00	35.00	37.50	165.00	3100.00	60.90
[31, 32]	C-2.5x15-S3	8.00	25.00	300.00	34.00	35.00	37.50	165.00	3100.00	58.10
[25]	Lb40X12_a	5.00	22.00	40.00	25.03	22.02	13.86	156.10	2879.00	19.93
[25]	Lb40X12_b	5.00	22.00	40.00	25.03	22.02	13.86	156.10	2879.00	19.81
[25]	Lb70X12_a	5.00	22.00	70.00	25.03	22.02	13.86	156.10	2879.00	31.43

Continued on next page

*Continued from previous page*

Paper ID	Specimen ID	$b_g$ [mm]	$d_g$ [mm]	$L_b$ [mm]	$f_{cm}$ [MPa]	$p_f$ [mm]	$A_f$ [mm <sup>2</sup> ]	$E_f$ [GPa]	$f_{fu}$ [MPa]	$F_{fmax}$ [kN]
[25]	Lb70X12_b	5.00	22.00	70.00	25.03	22.02	13.86	156.10	2879.00	29.40
[25]	Lb40X6_a	5.00	22.00	40.00	25.03	22.02	13.86	156.10	2879.00	18.58
[25]	Lb40X6_b	5.00	22.00	40.00	25.03	22.02	13.86	156.10	2879.00	18.59
[25]	Lb70X6_a	5.00	22.00	70.00	25.03	22.02	13.86	156.10	2879.00	27.70
[25]	Lb70X6_b	5.00	22.00	70.00	25.03	22.02	13.86	156.10	2879.00	26.74
[25]	Lb90X0_a	5.00	22.00	90.00	25.03	22.02	13.86	156.10	2879.00	27.92
[25]	Lb90X0_b	5.00	22.00	90.00	25.03	22.02	13.86	156.10	2879.00	27.80
[25]	Lb50X0_a	5.00	22.00	50.00	25.03	42.80	28.00	165.00	1850.00	31.27
[25]	Lb50X0_b	5.00	22.00	50.00	25.03	42.80	28.00	165.00	1850.00	31.55
[34]	Rectangular_200	6.00	25.00	200.00	34.86	42.80	28.00	165.00	2300.00	24.00
[34]	Rectangular_250	6.00	25.00	250.00	34.86	42.80	28.00	165.00	2300.00	31.00
Adhesive/Concrete interface failure mode, A/C (17 specimens)										
[23]	C-2.5x15-S-1	8	25	300	18.4	35	37.5	182	2863	52.97
[23]	C-2.5x15-S-2	8	25	300	18.4	35	37.5	182	2863	56.03
[23]	C-2.5x15-S-3	8	25	300	18.4	35	37.5	182	2863	46.26

*Continued on next page*

Continued from previous page

Paper ID	Specimen ID	$b_g$ [mm]	$d_g$ [mm]	$L_b$ [mm]	$f_{cm}$ [MPa]	$p_f$ [mm]	$A_f$ [mm <sup>2</sup> ]	$E_f$ [GPa]	$f_{fu}$ [MPa]	$F_{fmax}$ [kN]
[35]	C1.4x10S-1	4.64	15.54	300	34.8	22.8	14	165	1850	36.6
[35]	C1.4x10S-2	4.64	15.54	300	34.8	22.8	14	165	1850	39.4
[35]	C1.4x10S-3	4.64	15.54	300	34.8	22.8	14	165	1850	41.4
[35]	C2.5x15S	7.65	23.56	300	34.8	35	37.5	165	3100	49.6
[35]	C2.5x15S	7.65	23.56	300	34.8	35	37.5	165	3100	48.3
[35]	C2.5x15S	7.65	23.56	300	34.8	35	37.5	165	3100	48
[34]	Rectangular_300	6	25	300	34.86	42.8	28	165	2300	51
[26]**	TS2-6.0-C40	NA	45	350	38.8	32	60	153	2700	150
[36]**	DP600NS-1	6.4	19	152	NA	36	32	130	2500	43.6
[36]**	DP600NS-2	6.4	19	152	NA	36	32	130	2500	54.3
[36]**	DP600NS-3	6.4	19	152	NA	36	32	130	2500	50.7
[36]**	DP600NS-4	6.4	19	152	NA	36	32	130	2500	41.8
[36]**	DP600NS-5	6.4	19	152	NA	36	32	130	2500	48
[36]**	DP600NS-6	6.4	19	152	NA	36	32	130	2500	48

37

Notes: \* specimens not used in the analyses with SA formulation as in this guideline but used in the

594 analyses with SA by failure mode; \*\* specimens not used in the analyses with SA formulation as in the  
595 guideline nor in the analyses with SA by failure mode.

596 **References**

- 597 [1] Coelho M, Sena-Cruz J, Neves L. A review on the bond behavior of  
598 FRP NSM systems in concrete. *Construction and Building Materials*  
599 2015;93:1157–69. URL [http://dx.doi.org/10.1016/j.conbuildmat.  
600 2015.05.010](http://dx.doi.org/10.1016/j.conbuildmat.2015.05.010).
- 601 [2] Zhang S, Yu T, Chen G. Reinforced concrete beams strengthened in  
602 flexure with near-surface mounted (NSM) CFRP strips: Current status  
603 and research needs. *Composites Part B: Engineering* 2017;131:30–42.  
604 URL <http://dx.doi.org/10.1016/j.compositesb.2017.07.072>.
- 605 [3] Breveglieri M, Aprile A, Barros J. RC beams strengthened in shear using  
606 the Embedded Through-Section technique: Experimental results and  
607 analytical formulation. *Composites Part B: Engineering* 2016;89:266–  
608 81. URL <http://dx.doi.org/10.1016/j.compositesb.2015.11.023>.
- 609 [4] ACI. Guide for the design and construction of externally bonded FRP  
610 systems for strengthening concrete structures. 4402R-08; American Con-  
611 crete Institute, Farmington Hills, MI, USA; 2008.
- 612 [5] SA. Design handbook for RC structures retrofitted with FRP and metal  
613 plates: beams and slabs. HB 305-2008; Standards Australia GPO Box  
614 476, Sydney, NSW 2001, Australia; 2008.
- 615 [6] CEN. Eurocode 2: Design of concrete structures. EN 1992-1-1:2004 E;  
616 Comité Européen de Normalisation, Bruxelles; 2004.
- 617 [7] CEN. Eurocode 0: Basis of structural design. EN 1990:2002 E; Comité  
618 Européen de Normalisation, Bruxelles; 2002.

- 619 [8] Bianco V, Monti G, Barros J. Design formula to evaluate the NSM  
620 FRP strips shear strength contribution to a RC beam. *Composites Part*  
621 *B: Engineering* 2014;56:960–71. URL [http://dx.doi.org/10.1016/j.](http://dx.doi.org/10.1016/j.compositesb.2013.09.001)  
622 [compositesb.2013.09.001](http://dx.doi.org/10.1016/j.compositesb.2013.09.001).
- 623 [9] Lignola G, Jalayer F, Nardone F, Prota A, Manfredi G. Probabilistic de-  
624 sign equations for the shear capacity of RC members with FRP internal  
625 shear reinforcement. *Composites Part B: Engineering* 2014;67:199–208.  
626 URL <http://dx.doi.org/10.1016/j.compositesb.2014.07.007>.
- 627 [10] Bilotta A, Ludovico MD, Nigro E. FRP-to-concrete interface debond-  
628 ing: experimental calibration of a capacity model. *Composites Part B:*  
629 *Engineering* 2011;42(6):1539–53. URL [http://dx.doi.org/10.1016/](http://dx.doi.org/10.1016/j.compositesb.2011.04.016)  
630 [j.compositesb.2011.04.016](http://dx.doi.org/10.1016/j.compositesb.2011.04.016).
- 631 [11] Bilotta A, Faella C, Martinelli E, Nigro E. Design by testing proce-  
632 dure for intermediate debonding in EBR FRP strengthened RC beams.  
633 *Engineering Structures* 2013;46:147–54. URL [http://dx.doi.org/10.](http://dx.doi.org/10.1016/j.engstruct.2012.06.031)  
634 [1016/j.engstruct.2012.06.031](http://dx.doi.org/10.1016/j.engstruct.2012.06.031).
- 635 [12] Monti G, Alessandri S, Santini S. Design by testing: a procedure for the  
636 statistical determination of capacity models. *Construction and Building*  
637 *Materials* 2009;23(4):1487–94. URL [http://dx.doi.org/10.1016/j.](http://dx.doi.org/10.1016/j.conbuildmat.2008.07.016)  
638 [conbuildmat.2008.07.016](http://dx.doi.org/10.1016/j.conbuildmat.2008.07.016).
- 639 [13] Monti G, Santini S. Reliability-based calibration of partial safety co-  
640 efficients for fiber-reinforced plastic. *Journal of Composites for Con-*



- 641       struction 2002;6(3):162–7. URL [http://dx.doi.org/10.1061/\(ASCE\)](http://dx.doi.org/10.1061/(ASCE)1090-0268(2002)6:3(162))  
642       [1090-0268\(2002\)6:3\(162\)](http://dx.doi.org/10.1061/(ASCE)1090-0268(2002)6:3(162)).
- 643 [14] Carrara P, Freddi F. Statistical assessment of a design formula for  
644       the debonding resistance of FRP reinforcements externally glued on  
645       masonry units. *Composites Part B: Engineering* 2014;66:65–82. URL  
646       <http://dx.doi.org/10.1016/j.compositesb.2014.04.032>.
- 647 [15] Gomes S, Neves L, Dias-da Costa D, Fernandes P, Júlio E. Probabilistic models for mechanical properties of prefabricated CFRP. In:  
648       11th fiber reinforced polymers for reinforced concrete structures (FR-  
649       PRCS11), Guimarães, Portugal. 2013,.
- 651 [16] JCSS. Probabilistic model code. The Joint Committee on Structural  
652       Safety; 2001.
- 653 [17] CNR. Istruzioni per la progettazione, l'esecuzione ed il controllo di  
654       interventi di consolidamento statico mediante l'utilizzo di compositi fi-  
655       brorinforzati. CNR-DT 200 R1/2012; National Research Council, Rome,  
656       Italy; 2012.
- 657 [18] CSA. Canadian highway bridge design code. CAN/CSA S6-06; Cana-  
658       dian Standards Association, Canada; 2006.
- 659 [19] Atadero RA, Karbhari VM. Probabilistic based design for FRP strength-  
660       ening of reinforced concrete. *Special Publication (ACI)* 2005;230:723–42.
- 661 [20] Zureick A, Bennett R, Ellingwood B. Statistical characterization of fiber-  
662       reinforced polymer composite material properties for structural design.

- 663 Journal of Structural Engineering 2006;132(8):1320–7. URL [http://](http://dx.doi.org/10.1061/(ASCE)0733-9445(2006)132:8(1320))  
664 [dx.doi.org/10.1061/\(ASCE\)0733-9445\(2006\)132:8\(1320\)](http://dx.doi.org/10.1061/(ASCE)0733-9445(2006)132:8(1320)).
- 665 [21] Zhang S, Yu T, Chen G. Reliability analysis of tensile strengths  
666 using Weibull distribution in glass/epoxy and carbon/epoxy compos-  
667 ites. Composites Part B: Engineering 2018;133:129–44. URL [https:](https://doi.org/10.1016/j.compositesb.2017.09.002)  
668 [//doi.org/10.1016/j.compositesb.2017.09.002](https://doi.org/10.1016/j.compositesb.2017.09.002).
- 669 [22] Seracino R, Jones N, Ali M, Page M, Oehlers D. Bond strength of  
670 near-surface mounted FRP strip-to-concrete joints. Journal of Compos-  
671 ites for Construction 2007;11(4):401–9. URL [http://dx.doi.org/10.](http://dx.doi.org/10.1061/(ASCE)1090-0268(2007)11:4(401))  
672 [1061/\(ASCE\)1090-0268\(2007\)11:4\(401\)](http://dx.doi.org/10.1061/(ASCE)1090-0268(2007)11:4(401)).
- 673 [23] Bilotta A, Ceroni F, Di Ludovico M, Nigro E, Pecce M, Man-  
674 fredi G. Bond efficiency of EBR and NSM FRP systems for  
675 strengthening concrete members. Journal of Composites for Construc-  
676 tion 2011;15(5):757–72. URL [http://dx.doi.org/10.1061/\(asce\)cc.](http://dx.doi.org/10.1061/(asce)cc.1943-5614.0000204)  
677 [1943-5614.0000204](http://dx.doi.org/10.1061/(asce)cc.1943-5614.0000204).
- 678 [24] Kalupahana W. Anchorage and bond behaviour of near surface mounted  
679 fibre reinforced polymer bars. Phd thesis; University of Bath, United  
680 Kingdom; 2009.
- 681 [25] Macedo L, Costa I, Barros J. Assessment of the influence of the adhesive  
682 properties and geometry of CFRP laminates in the bond behavior. In:  
683 BE2008 - Betão Estrutural 2008. Guimarães, Portugal. 2008,.
- 684 [26] Oehlers DJ, Haskett M, Wu C, Seracino R. Embedding NSM FRP  
685 plates for improved IC debonding resistance. Journal of Composites for

- 686 Construction 2008;12(6):635–42. URL <http://dx.doi.org/10.1061/>  
687  [\(asce\)1090-0268\(2008\)12:6\(635\)](http://dx.doi.org/10.1061/(asce)1090-0268(2008)12:6(635)).
- 688 [27] Thorenfeldt E. Bond capacity of CFRP strips glued to concrete in sawn  
689 slits. In: FRPRCS-8, Patras, Greece. 2007,.
- 690 [28] Mitchell P. Freeze-thaw and sustained load durability of near surface  
691 mounted FRP strengthened concrete. MSc Thesis, Queens University,  
692 Canada; 2010.
- 693 [29] Rashid R, Oehlers DJ, Seracino R. IC debonding of FRP NSM and  
694 EB retrofitted concrete: plate and cover interaction tests. Journal of  
695 Composites for Construction 2008;12(2):160–7. URL [http://dx.doi.](http://dx.doi.org/10.1061/(asce)1090-0268(2008)12:2(160))  
696 [org/10.1061/\(asce\)1090-0268\(2008\)12:2\(160\)](http://dx.doi.org/10.1061/(asce)1090-0268(2008)12:2(160)).
- 697 [30] Seo SY, Feo L, Hui D. Bond strength of near surface-mounted FRP plate  
698 for retrofit of concrete structures. Composite Structures 2013;95:719–27.  
699 URL <http://dx.doi.org/10.1016/j.compstruct.2012.08.038>.
- 700 [31] Palmieri A, Matthys S, Barros J, Costa I, Bilotta A, Nigro E, et al.  
701 Bond of NSM FRP strengthened concrete: round robin test initiative.  
702 In: CICE 2012, Rome, Italy. 2012,.
- 703 [32] Palmieri A, Matthys S, Taerwe L. Double bond shear tests on NSM  
704 FRP strengthened members. In: CICE 2012, Rome, Italy. 2012,.
- 705 [33] Teng JG, De Lorenzis L, Wang B, Li R, Wong T, Lam L. Debonding  
706 failures of RC beams strengthened with near surface mounted CFRP  
707 strips. Journal of Composites for Construction 2006;10(2):92–105. URL  
708 [http://dx.doi.org/10.1061/\(ASCE\)1090-0268\(2006\)10:2\(92\)](http://dx.doi.org/10.1061/(ASCE)1090-0268(2006)10:2(92)).

- 709 [34] Capozucca R. Analysis of bond-slip effects in RC beams strengthened  
710 with NSM CFRP rods. *Composite Structures* 2013;102:110–23. URL  
711 <http://dx.doi.org/10.1016/j.compstruct.2013.02.024>.
- 712 [35] Barros J, Costa I. Bond tests on near surface reinforcement strengthen-  
713 ing for concrete structures. Tech. Rep.; Civil Engineering Department,  
714 University of Minho, Guimarães, Portugal; 2010.
- 715 [36] Shield C, French C, Milde E. The effect of adhesive type on the bond  
716 of NSM tape to concrete. In: FRPRCS7, Kansas City, Missouri, USA.  
717 2005, p. 355–72.

718 **List of Figures**

719     1     Example of a direct pullout test specimen and its possible local  
720           failure modes. . . . . 46  
721     2     Design point and reliability index in the normalized space ac-  
722           cording to FORM. . . . . 47  
723     3     Probability density function of the error  $\delta$  associated with each  
724           limit state theoretical resistance function. . . . . 48  
725     4     Failure modes (FM) obtained in the experimental tests *versus*  
726           its prediction using the theoretical resistance model defined  
727           in: (a) ACI guideline; (b) SA guideline. . . . . 49  
728     5     Experimental *versus* predicted maximum pullout force consid-  
729           ering the specimens separately by experimental failure mode  
730           (FM) and applying the corresponding limit state function us-  
731           ing: (a) ACI guideline; (b) SA guideline. . . . . 50  
732     6     Histograms of the predictions errors for the resistance models  
733           of: (a) ACI guideline; (b) SA guideline; (c) ACI modified. . . . 51

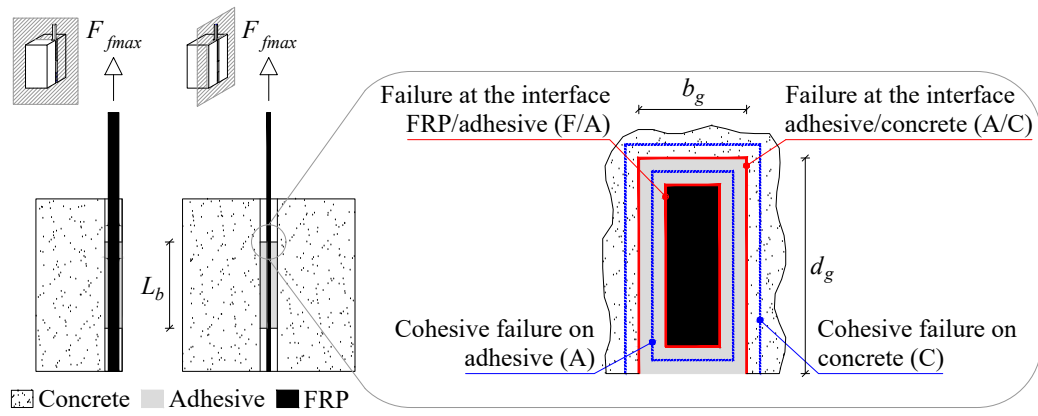


**Fig. 1.** Example of a direct pullout test specimen and its possible local failure modes.

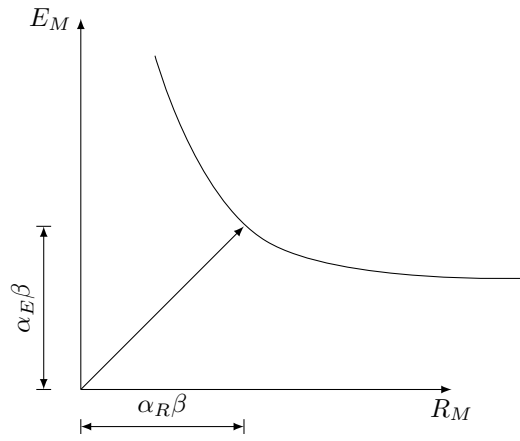


**Fig. 2.** Design point and reliability index in the normalized space according to FORM.

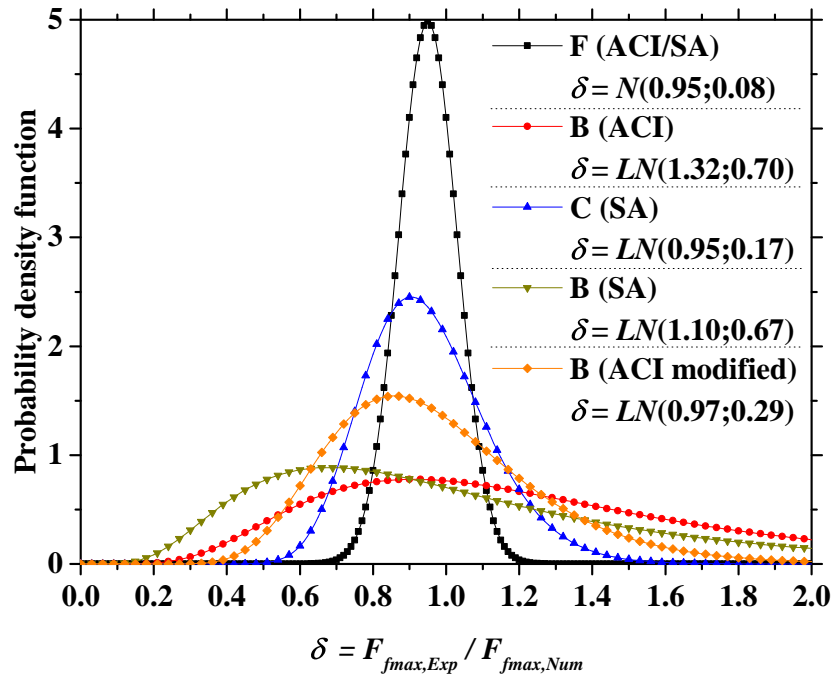


**Fig. 3.** Probability density function of the error  $\delta$  associated with each limit state theoretical resistance function.



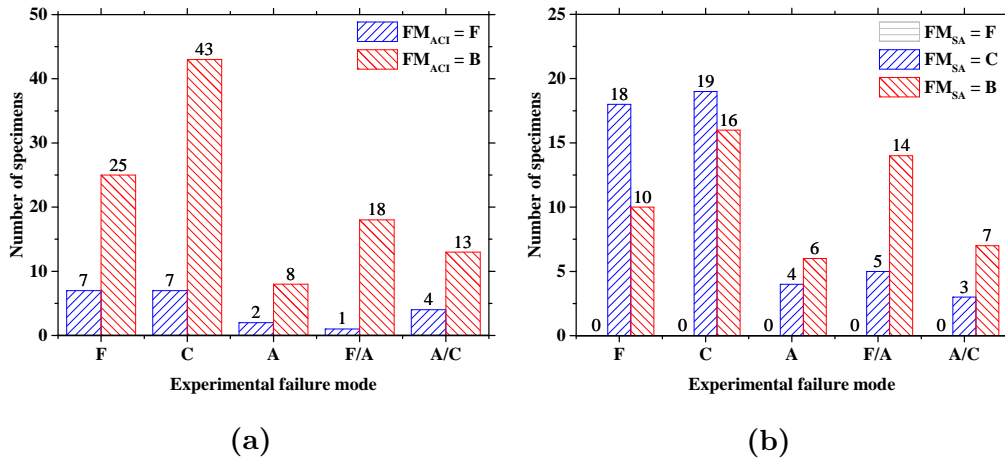


**Fig. 4.** Failure modes (FM) obtained in the experimental tests *versus* its prediction using the theoretical resistance model defined in: (a) ACI guideline; (b) SA guideline.

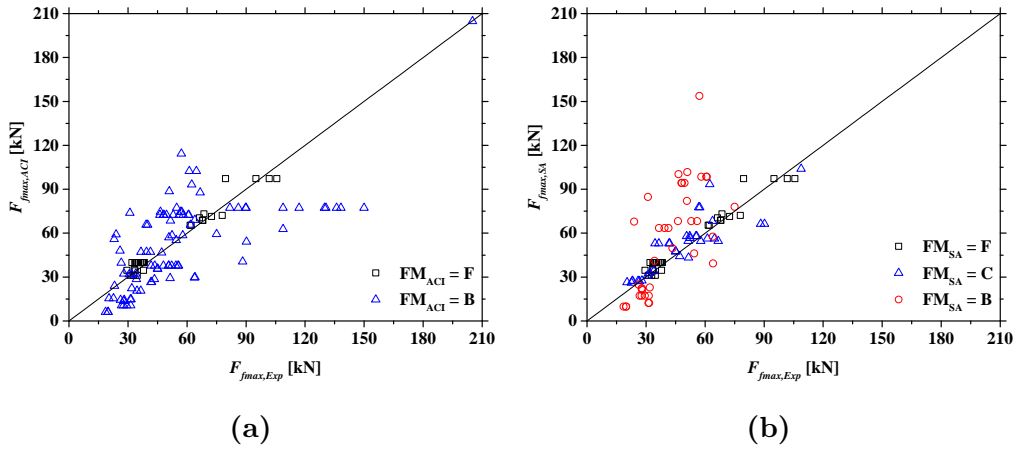
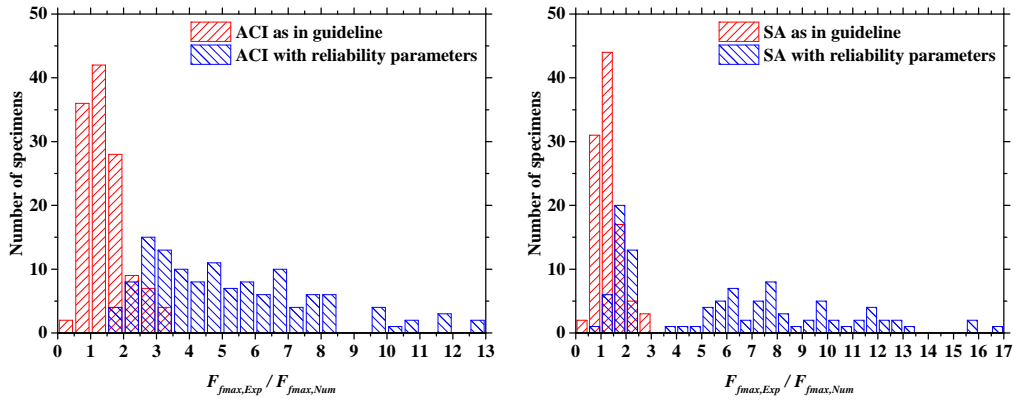
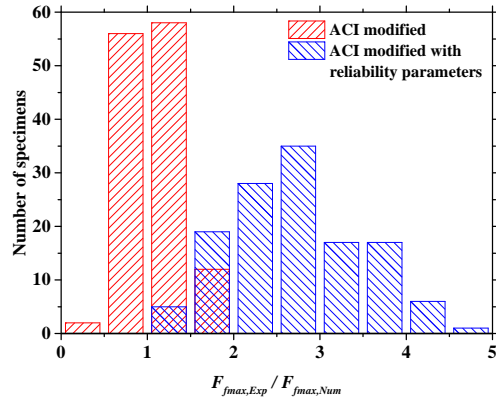


**Fig. 5.** Experimental *versus* predicted maximum pullout force considering the specimens separately by experimental failure mode (FM) and applying the corresponding limit state function using: (a) ACI guideline; (b) SA guideline.



(a)

(b)



(c)

**Fig. 6.** Histograms of the predictions errors for the resistance models of: (a) ACI guideline; (b) SA guideline; (c) ACI modified.

734 **List of Tables**

735     1     Summary of ACI and SA formulations to estimate NSM FRP  
736           systems bond strength. . . . . 53  
737     2     Results obtained in the partial safety factors method. . . . . 54  
738     3     Results obtained in the reliability analyses of SA limit states  
739           depending on the concrete class. . . . . 55

**Table 1.** Summary of ACI and SA formulations to estimate NSM FRP systems bond strength.

Parameter	ACI as defined in its guideline	SA as defined in its guideline
Development length [ $L_d$ ]	$(A_f f_{fd}) / (p_f \tau_{avg})$	$\pi / \left[ 2 \sqrt{(\tau_{max} L_{per}) / (\delta_{max} E_f A_f)} \right]$
Maximum pullout force [ $F_{fmax}$ ]	$\begin{cases} A_f f_{fd} & \text{if } L_b \geq L_d \\ A_f f_{fd} \frac{L_b}{L_d} & \text{if } L_b < L_d \end{cases}$	$\begin{cases} \sqrt{\tau_{max} \delta_{max} L_{per} E_f A_f} \leq A_f f_{fd} & \text{if } L_b \geq L_d \\ \sqrt{\tau_{max} \delta_{max} L_{per} E_f A_f} \frac{L_b}{L_d} \leq A_f f_{fd} & \text{if } L_b < L_d \end{cases}$
Other relevant information	$\tau_{avg} = 6.9 \text{ MPa}$	$\tau_{max} = (0.8 + 0.078 \varphi_{per}) f_c^{0.6}$ $\delta_{max} = (0.73 \varphi_{per}^{0.5} f_c^{0.67}) / \tau_{max}$ $\varphi_{per} = (d_g + 1) / (b_g + 2)$ $L_{per} = 2(d_g + 1) + b_g + 2$

**Table 2.** Results obtained in the partial safety factors method.

Limit state	Step in the partial safety factors method described in section 1 <sup>1</sup>				
	(i)		(iii)	(v)	(vi)
	Theoretical resistance function ( $R_t$ )	Random variables	Probabilistic resistance function distribution ( $R$ )	Design resistance function ( $R_d$ )	Safety factors
F (ACI/SA)	Eq. 10	$f_{fu}$	$\frac{R}{A_f} \sim N(2554.33; 298.18)^2$	$A_f \frac{f_{fk}}{\gamma_f}$	$\gamma_f = 1.4$
B (ACI)	Eq. 11	-	$\frac{R}{6.9L_b p_f} \sim LN(1.32; 0.70)^3$	$\tau_d L_b p_f$	$\tau_d = 1.77$
C (SA)	Eq. 12	$E_f; f_c$	$\frac{R}{\sqrt{0.73\varphi_{per}^{0.5} L_{per} A_f}} \sim^{2,4}$	$\eta_c \sqrt{0.73\varphi_{per}^{0.5} \left(\frac{f_{ck}}{\gamma_c}\right)^{0.67} L_{per} E_f A_f}$	<sup>4</sup>
B (SA)	Eq. 13	$f_c$	$\frac{R}{\frac{2L_b}{\pi} (0.8 + 0.078\varphi_{per}) L_{per}} \sim^{2,4}$	$\eta_b \frac{2L_b}{\pi} (0.8 + 0.078\varphi_{per}) L_{per} \left(\frac{f_{ck}}{\gamma_c}\right)^{0.6}$	<sup>4</sup>
B (ACI modified)	Eq. 14	-	$\frac{R}{162\left(\frac{A_f}{p_f L_b}\right)^{0.55} L_b p_f} \sim LN(0.97; 0.29)^3$	$\eta 162 \left(\frac{A_f}{p_f L_b}\right)^{0.55} L_b p_f$	$\eta = 0.38$

<sup>1</sup> step (ii) is depicted in Fig. 3 while step (iv) was achieved by applying Eq. 5 to each distribution of step (iii).

<sup>2</sup> joint probability obtained in  $10^6$  Monte Carlo simulations using the error  $\delta$  and the existing random variables.

<sup>3</sup> equal to the error probability distribution (see Fig. 3) since that is the only random variable.

<sup>4</sup> see Table 3.

**Table 3.** Results obtained in the reliability analyses of SA limit states depending on the concrete class.

Concrete class	Concrete cohesive failure limit state		Debonding limit state	
	Probabilistic resistance function model	$\eta_c$	Probabilistic resistance function model	$\eta_b$
C12/15	$LN(1088.39; 197.8)$	0.73	$LN(6.62; 4.06)$	0.29
C16/20	$LN(1156.37; 210.15)$	0.71	$LN(7.38; 4.54)$	0.27
C20/25	$LN(1217.96; 220.92)$	0.69	$LN(8.08; 4.96)$	0.26
C25/30	$LN(1287.07; 233.71)$	0.68	$LN(8.92; 5.48)$	0.25
C30/37	$LN(1348.87; 244.79)$	0.67	$LN(9.73; 5.98)$	0.25
C35/45	$LN(1406.82; 255.2)$	0.66	$LN(10.47; 6.44)$	0.24
C40/50	$LN(1458.9; 264.79)$	0.66	$LN(11.2; 6.89)$	0.24
C45/55	$LN(1507.47; 273.62)$	0.65	$LN(11.88; 7.29)$	0.24
C50/60	$LN(1553.57; 281.64)$	0.65	$LN(12.53; 7.71)$	0.23
C55/67	$LN(1597.68; 289.77)$	0.65	$LN(13.18; 8.12)$	0.23

740 **Notation**

741 The following acronyms and symbols are used in this paper:

Acronyms

<i>A</i>	Adhesive cohesive failure mode
<i>ACI</i>	American concrete institute guideline
<i>B</i>	Debonding failure mode (This includes C, A, F/A and A/C in the case of ACI, and A, F/A and A/C in the case of SA)
<i>C</i>	Concrete cohesive failure mode
<i>(C)FRP</i>	(Carbon) Fibre reinforced polymer
<i>EC</i>	Eurocode
<i>F</i>	FRP rupture failure mode
<i>NSM</i>	Near-surface mounted technique
<i>R</i>	Probabilistic resistance function
$R_e$	Experimental resistance value
$R_t$	Theoretical limit state resistance function
$R_d$	Design value of the limit state resistance function
<i>SA</i>	Standards Australia guideline
<i>A/C</i>	Adhesive/concrete interface failure mode
<i>F/A</i>	FRP/adhesive interface failure mode



## Symbols

$\delta$	Error
$\delta_d$	Design maximum bond slip
$\delta_{max}$	Maximum bond slip
$\gamma_c$	Concrete partial safety factor
$\gamma_f$	FRP partial safety factor
$\eta_b$	Debonding limit state global safety factor (SA guideline)
$\eta_c$	Concrete failure limit state global safety factor (SA guideline)
$\varphi_{per}$	Failure perimeter ratio
$\tau_d$	Design bond strength
$\tau_{avg}$	Average bond strength
$\tau_{max}$	Maximum bond strength
$A_f$	FRP cross-section area
$b_g$	Groove width
$d_g$	Groove depth
$E_f$	FRP modulus of elasticity
$f_c, f_{cm}, f_{ck}$	Concrete cylinder compressive strength, mean and characteristic values, respectively
$F_{fmax}$	Maximum pullout force installed in the FRP
$F_{fmax,d}$	Design maximum pullout force installed in the FRP
$f_{fu}, f_{fk}, f_d$	FRP tensile strength ultimate, characteristic and design values, respectively
$L_b$	Bonded length
$L_d$	Development length
$L_{per}$	SA failure plane perimeter
$p_f$	FRP perimeter